

Selective Catalytic Reduction of NO with Propene over Au/CeO₂/Al₂O₃ Catalysts

Xinkui Wang^{1,2}, Aiqin Wang¹, Xiaodong Wang¹, Xuefeng Yang² and Tao Zhang^{1*}

¹ State Key Laboratory of Catalysis, Dalian Institute of Chemical Physics, Chinese Academy of Sciences, Dalian 116023, China. E-mail: taozhang@dicp.ac.cn

² Laboratory of Plasma Physical Chemistry, Dalian University of Technology, Dalian 116023, China

Abstract

Selective catalytic reduction of NO by propene under an oxygen-rich atmosphere has been investigated over Au/CeO₂, Au/CeO₂/Al₂O₃ and Au/Al₂O₃ catalysts prepared by deposition-precipitation. The results demonstrated that Au/16%CeO₂/Al₂O₃ had good low-temperature activity, selectivity towards N₂ and stability, which is superior to that of Pt/Al₂O₃. It was also found that adding 2% water vapour to the feed stream enhanced the NO conversions at low temperatures while the presence of 20 ppm SO₂ increased NO conversions at higher temperatures. It is particularly interesting that under the simultaneous presence of 2% water vapour and 20 ppm SO₂, the NO conversions to N₂ were significantly increased and the temperature window was widened significantly. The catalysts were characterized by X-ray diffraction (XRD), high resolution transmission electron microscopy coupled with energy dispersive X-ray spectroscopy (HRTEM-EDX) and temperature-programmed reduction (H₂-TPR) techniques. Both XRD and HRTEM revealed that CeO₂ was highly dispersed on the alumina support, and HRTEM combined with EDX showed that gold particles were preferentially deposited on those highly dispersed CeO₂ particles. The gold deposition made CeO₂ more reducible and interaction between gold and those highly dispersed CeO₂ particles became stronger than that with the bulk CeO₂, and this interaction is probably responsible for the superior catalytic performance of the Au/CeO₂/Al₂O₃.

Keywords

Gold, Ceria, SCR, NO, Propene

Introduction

Selective catalytic reduction of NO by hydrocarbons in the presence of excess oxygen (HC-SCR) is considered as a potentially promising way to remove NO_x from automobile exhaust. Among the various catalysts investigated, supported platinum-based catalysts have shown the highest activities at low temperatures (between 200°C and 350°C) in the tests on a diesel engine working in an urban cycle (1). However, the high selectivity to N₂O over the Pt-based catalysts largely limited their applications, since N₂O contributes significantly to a greenhouse effect. Consequently, much work has been done to increase the selectivity to N₂ and limit the production of N₂O at low temperatures by varying the nature of the support, the preparation method or by using various hydrocarbons as the reductants (2-5).

In the last decade, catalysis by gold has been the hotspot in the heterogeneous catalysis field due to its exceptionally high activities at low temperatures, in particular for CO oxidation (6). We believe that such a unique feature of gold catalysts has a close relationship with the weak adsorption of most reactant molecules on gold nanoparticles. Another advantage that the use of gold catalysts offer compared to Pt catalysts is the lower cost and greater price stability of gold, which is important in their application for automobile emission control. However, in contrast with the extensively studied low-temperature CO oxidation, NO reduction with hydrocarbons under an oxygen-rich atmosphere has been less studied over nanogold catalysts although oxide supported gold nanoparticles have been found to give good catalytic performances at both high and relatively low temperature (7,8). Among the various catalysts investigated, Au/ZnO prepared by co-precipitation has shown the best low temperature catalytic activity, which gives a maximum NO conversion of 25% at 250°C (7). However, over Au/ZnO, N₂O is also formed and ZnO support is less thermally stable compared with alumina when exposed to high-temperature emissions. Therefore, ZnO is not the best choice as a catalyst support for automotive emission control. On the other hand, it is well known that ceria-alumina is one of the best supports of three way catalysts used for the elimination of pollutants in automobile exhausts onto which precious metals (typically Rh, Pt and/or Pd) are dispersed (9). Ceria is a structural promoting component. It enhances the metal dispersion and participates in the stabilization of the alumina support against thermal sintering (10,11). On the other hand, the addition of ceria to alumina induces a modification of the electronic density of the aluminium cations, implying a change in the acid-base properties of the support surface (12). In addition, the well established catalytic and redox properties of the Ce³⁺/Ce⁴⁺ couple, makes CeO₂/Al₂O₃ a suitable support for obtaining

well dispersed and active gold catalyst for the oxidation of CO and volatile organic compounds (13,14).

In the present work, which has the objective of combining the above advantages of gold nanocatalysts with those of the $\text{CeO}_2/\text{Al}_2\text{O}_3$ support, we attempt to prepare highly dispersed gold nanoparticles on $\text{CeO}_2/\text{Al}_2\text{O}_3$ support and apply it to the HC-SCR reaction. We firstly prepared four gold-containing catalysts, Au/CeO_2 , $\text{Au}/\text{Al}_2\text{O}_3$, $\text{Au}/5\%\text{CeO}_2/\text{Al}_2\text{O}_3$ and $\text{Au}/16\%\text{CeO}_2/\text{Al}_2\text{O}_3$ by deposition-precipitation. The catalytic activity tests showed that $\text{Au}/16\%\text{CeO}_2/\text{Al}_2\text{O}_3$ exhibited a good low-temperature activity and a high selectivity to N_2 for NO reduction with propene under an oxygen-rich atmosphere. Various characterization techniques including XRD, TEM, EDX, and H_2 -TPR were employed to characterize the $\text{Au}/\text{CeO}_2/\text{Al}_2\text{O}_3$ catalysts.

Experimental

Preparation of the samples

The starting $\gamma\text{-Al}_2\text{O}_3$ powder was made in our laboratory and had a BET surface area of $228\text{m}^2/\text{g}$. CeO_2 powder was obtained by thermal decomposition of cerous nitrate at 650°C in the air for 4h, giving a BET surface area of $58\text{m}^2/\text{g}$. The composite support $\text{CeO}_2/\text{Al}_2\text{O}_3$ with various CeO_2 loadings was prepared by impregnation of the $\gamma\text{-Al}_2\text{O}_3$ with an aqueous solution of cerous nitrate. Following impregnation, the sample was dried at 120°C for 6h and then calcined in air at 500°C for 4h. Gold-containing catalysts were prepared by deposition-precipitation. An appropriate volume of an aqueous solution of HAuCl_4 ($1.6 \times 10^{-3}\text{M}$) was adjusted to $\text{pH} = 7$ by dropwise addition of 1N NaOH solution. The resulting solution was heated to 70°C , and then 2g of the support powder (Al_2O_3 , CeO_2 or $\text{CeO}_2/\text{Al}_2\text{O}_3$) was added. The resulting mixture was continuously stirred at 70°C for 16h. After filtration and repeated washing until no Cl^- could be detected, the solid sample was dried at 120°C for 12h and calcined at 500°C in $20\%\text{O}_2/\text{He}$ for 1h.

Characterization techniques

BET specific surface areas were measured by nitrogen adsorption at -196°C on a Micromeritics ASAP 2010 apparatus. Before analysis, the samples were degassed at 350°C for 4h.

Gold contents of the catalyst samples were determined by inductively coupled plasma spectrometer (ICP-AES).

XRD patterns were obtained on a Rigaku D/MAX-2500/PC powder X-ray diffractometer using a Cu K_α radiation source ($\lambda = 0.15432\text{ nm}$), operated at 40kV and 250mA. The samples were scanned in the 2θ range from 10 to 80°C .

Gold particle size was examined using HRTEM (FEI TECNAI G² F30, operated at 320 kV). The samples were ultrasonically dispersed in ethanol and dropped on a copper grid coated with a carbon film.

H_2 -TPR experiments were carried out on a Micromeritics Auto Chem II 2920. 0.15g of the sample was pretreated at 200°C in an Ar stream for 1h in order to remove surface

contaminants. After cooling to room temperature under Ar, the gas flow was switched to $10\%\text{H}_2/\text{Ar}$ at a flow rate of 30ml/min, and the temperature was raised at a rate of $10^\circ\text{C}/\text{min}$ up to 1000°C . The consumption of H_2 was recorded with TCD.

Catalytic measurements

Catalytic activity measurements were carried out using a fixed-bed flow reactor. A reactant gas mixture containing 1000ppm NO, 1000ppm C_3H_6 , 5% O_2 , 0 or 2% H_2O and 0 or 20ppm SO_2 in helium passed through 0.15g catalyst at a flow rate of 100mL/min, corresponding to a space velocity of $30,000\text{h}^{-1}$. The effluent gas mixture was analysed using an on-line gas chromatograph (HP6890) equipped with TCD and FID.

Results and Discussion

Effect of CeO_2 addition on the gold loading

Table 1 indicates the gold loadings (determined by ICP-AES) and BET surface areas of the catalyst samples. We noticed that the actual gold contents in the four catalyst samples are all far lower than the desired value (2.4 wt%), indicating that a low loading efficiency resulted from the deposition-precipitation process. Moreover, with the addition of CeO_2 to the Al_2O_3 support, the gold loading increased from 0.6 wt% to 1.0%, and it was 1.4% on the pure CeO_2 support. This can be explained by the more basic character of CeO_2 compared to alumina. In fact, it has been described that when cerium is in direct contact with alumina, cerium-oxygen bonds are more basic than aluminate-type ligands since Ce is less electronegative than Al (15,16). In this respect, the basicity of ceria may contribute to the difference in the gold loading. On the other hand, the higher gold loading on the ceria support also implies a stronger interaction between gold particles and the ceria support, probably due to the oxygen vacancy of the ceria support (17). Clearly, addition of ceria to the alumina support can significantly modify its surface nature, inducing more gold particles to be deposited on it.

Gold particle size distribution on the $\text{Au}/\text{CeO}_2/\text{Al}_2\text{O}_3$

Figure 1 depicts the wide-angle XRD patterns of the samples. For the Au/CeO_2 , a very weak and broad peak at 38.2° due to crystalline gold can be observed in addition to the diffraction lines of CeO_2 (Figure 1A), indicating a very small

Table 1

Gold loading and BET surface area of the samples.

Sample	Au wt%	S_{BET} (m^2/g)
Au/CeO_2	1.4	58
$\text{Au}/\text{Al}_2\text{O}_3$	0.6	227
$\text{Au}/5\%\text{CeO}_2/\text{Al}_2\text{O}_3$	0.9	226
$\text{Au}/16\%\text{CeO}_2/\text{Al}_2\text{O}_3$	1.0	190

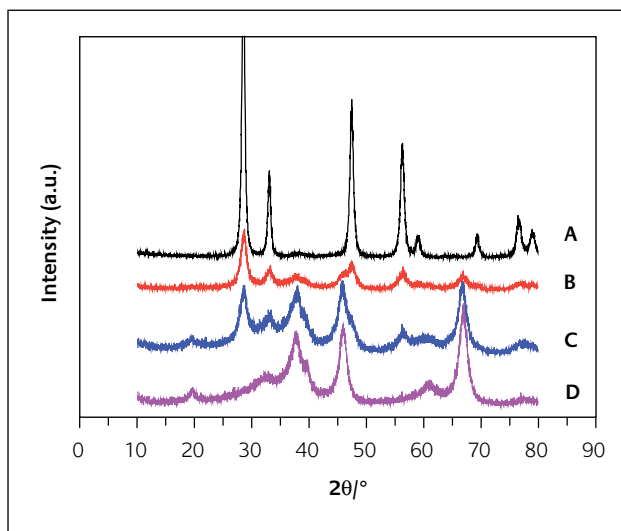


Figure 1

XRD patterns of 1.4% Au/CeO₂ (A), 1.0%Au/16%CeO₂/Al₂O₃ (B), 0.9% Au/5%CeO₂/Al₂O₃ (C) and 0.6%Au/Al₂O₃ (D).

gold particle size. For the other three samples with Al₂O₃ as the main component of the support (Figures 1B, C and D), we cannot observe gold diffraction lines because the strongest diffraction line of gold at 38.2° (111) coincidentally overlaps with the γ -Al₂O₃ diffraction line. On the other hand, compared with XRD peaks of Au/CeO₂, both the Au/5%CeO₂/Al₂O₃ and the Au/16%CeO₂/Al₂O₃ exhibited broadened CeO₂ peaks. From Scherrer's equation, ceria particle size was estimated to be about 13 nm in the Au/CeO₂ sample, while it was only about 7 nm on the Au/16%CeO₂/Al₂O₃ (Figure 1B). Thus, CeO₂ was highly dispersed on the Al₂O₃ support.

Figure 2 shows the HRTEM images of the Au/Al₂O₃ and the Au/16%CeO₂/Al₂O₃. From Figure 2A we can see that gold particles with a size of 3-5nm are highly dispersed

onto the alumina support. This is in agreement with the literature (18). However, for the Au/16%CeO₂/Al₂O₃ sample, it is difficult to distinguish gold particles from the ceria particles because of the high atomic weight of the cerium atom. From the HRTEM image (Figure 2B) of 1.0%Au/16%CeO₂/Al₂O₃, the ceria particles with a lattice fringe of 0.32 nm can be clearly observed (19), and the particle size of ceria is 6-8 nm, consistent with the XRD results. In addition, gold particles with a lattice fringe of 0.23 nm and a particle size of 3-5nm can be identified (19). To confirm the presence of gold particles on the ceria support, we performed the STEM (bright field) on the 1.0%Au/16%CeO₂/Al₂O₃ sample, as shown in Figure 3. The bright particles in the image correspond to the ceria or gold, while the dark parts are due to the alumina support. The EDX analysis on the selected bright spot shows that the bright spot is mainly composed of gold and ceria. In fact, examination on various parts of the image with EDX revealed that gold is always present associated with the ceria. This result implies that gold particles are preferentially deposited onto the ceria phase in the CeO₂/Al₂O₃ composite, again demonstrating the stronger interaction between gold and the ceria. The higher gold loading on the ceria-containing support also supports this conclusion. A similar conclusion was arrived at by Centeno et al (13,14) from EDX and XPS results.

H₂-TPR results

H₂-TPR profiles of the Au/CeO₂, Au/Al₂O₃, Au/5%CeO₂/Al₂O₃ and Au/16%CeO₂/Al₂O₃ are illustrated in Figure 4, and those of the corresponding supports are shown in Figure 5. The TPR profile of pure CeO₂ (Figure 5A) contains two peaks: a low temperature (LT) peak at T_{max} = 488°C assigned to the reduction of surface CeO₂ and a high temperature (HT) peak at T_{max} = 840°C due to the reduction of bulk ceria (20). When ceria was deposited onto the alumina support, the

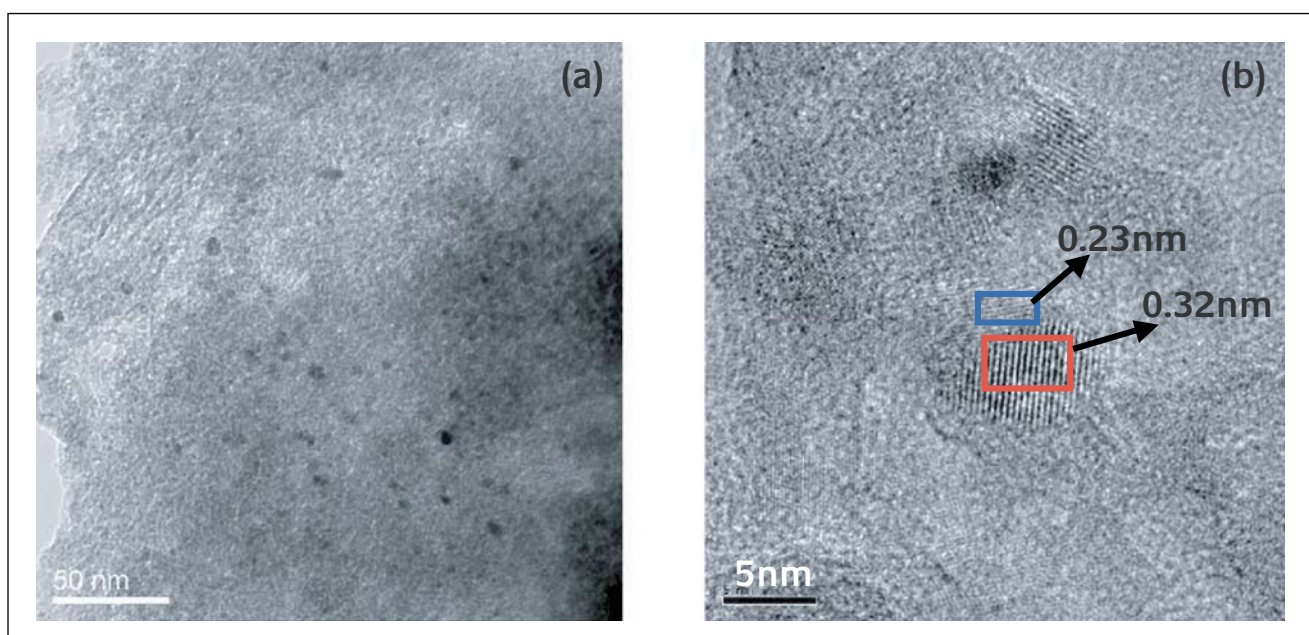


Figure 2

HRTEM photographs of 0.6% Au/Al₂O₃ (A) and 1.0%Au/16%CeO₂/Al₂O₃ (B).

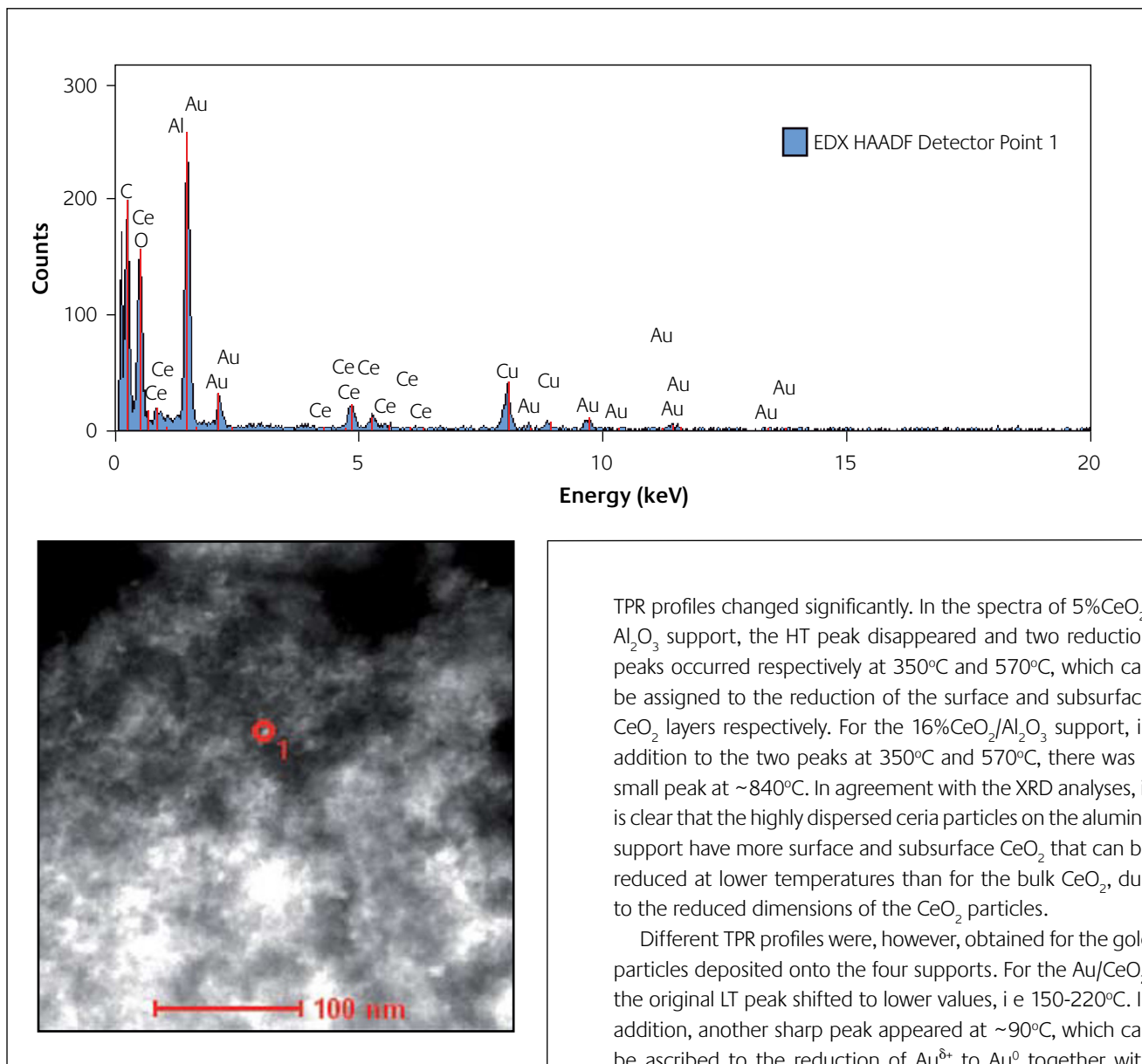


Figure 3
Typical STEM image and EDX analysis of 1.0% Au/16% CeO₂/Al₂O₃.

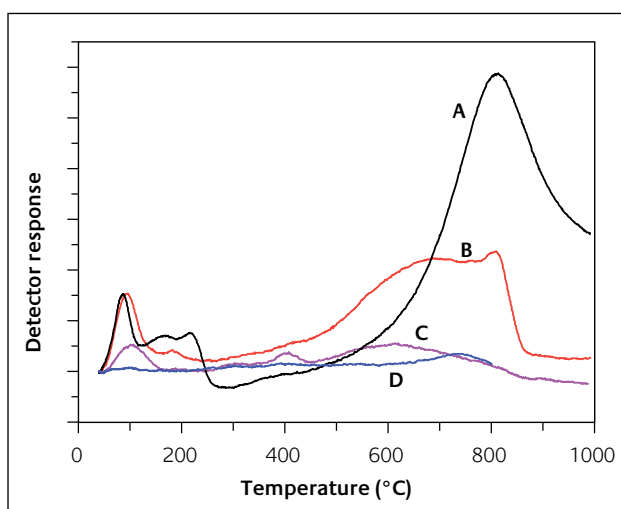


Figure 4
H₂-TPR profiles of 1.4% Au/CeO₂(A), 1.0% Au/16% CeO₂/Al₂O₃(B) 0.9% Au/5% CeO₂/Al₂O₃(C) and 0.6% Au/Al₂O₃(D).

TPR profiles changed significantly. In the spectra of 5%CeO₂/Al₂O₃ support, the HT peak disappeared and two reduction peaks occurred respectively at 350°C and 570°C, which can be assigned to the reduction of the surface and subsurface CeO₂ layers respectively. For the 16%CeO₂/Al₂O₃ support, in addition to the two peaks at 350°C and 570°C, there was a small peak at ~840°C. In agreement with the XRD analyses, it is clear that the highly dispersed ceria particles on the alumina support have more surface and subsurface CeO₂ that can be reduced at lower temperatures than for the bulk CeO₂, due to the reduced dimensions of the CeO₂ particles.

Different TPR profiles were, however, obtained for the gold particles deposited onto the four supports. For the Au/CeO₂, the original LT peak shifted to lower values, i.e. 150-220°C. In addition, another sharp peak appeared at ~90°C, which can be ascribed to the reduction of Au^{δ+} to Au⁰ together with the reduction of surface ceria (21-23). For the other two Au/CeO₂/Al₂O₃ catalysts, the reduction peaks of Au^{δ+} to Au⁰ as well as the reduction of surface ceria are also observed at ~100°C. Different from the Au/CeO₂/Al₂O₃ catalysts, when Au was deposited onto the pure Al₂O₃ support, no reduction peaks can be observed on the Au/Al₂O₃ within the whole investigated temperature range (Figure 4D), indicating the metallic state of Au. The presence of Au^{δ+} on the CeO₂-containing support reflects the strong interaction between gold and ceria. It has been reported that the high activity of Au/CeO₂/Al₂O₃ catalysts might be related to the capacity of Au nanoparticles to weaken the Ce-O bond. Thus, the mobility/reactivity of the surface lattice oxygen is increased by the presence of gold, and this even makes the gold particles, probably on the oxygen vacancies, oxidized to some extent (21,24).

Catalytic activity

In this work, we firstly compared the catalytic performances of gold particles on different supports: Al₂O₃, CeO₂, 5%CeO₂/Al₂O₃ and 16%CeO₂/Al₂O₃, for NO reduction with propene in

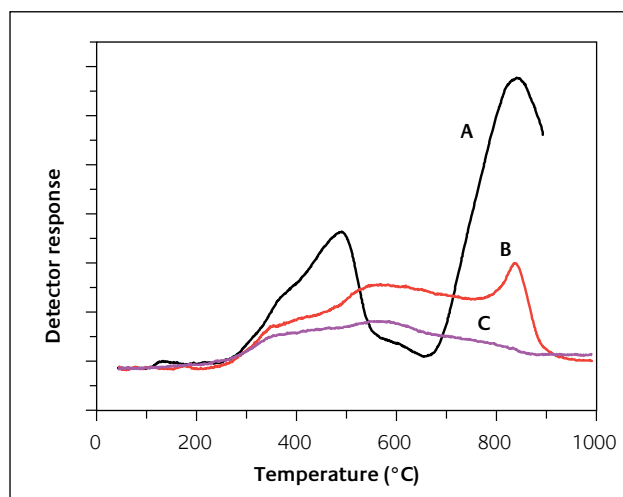
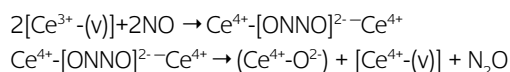


Figure 5

H₂-TPR profiles of CeO₂ (A), 16%CeO₂/Al₂O₃ (B) and 5%CeO₂/Al₂O₃ (C).

the presence of excess oxygen. Figure 6 (A, B, C) illustrates the conversions of NO to N₂ and N₂O and the conversions of C₃H₆ as a function of the reaction temperature. It is clear that Au/CeO₂ has a very low selectivity to N₂ but a comparatively high selectivity to N₂O. For example, the maximum NO conversion to N₂ was only 5% at 200 °C, while the conversion to N₂O reached 26% at 250 °C. In contrast, the catalytic performance of Au/Al₂O₃ is very different from that of Au/CeO₂. NO conversion to N₂ was at the highest value of 47% at 450 °C on the Au/Al₂O₃, while only a small amount of N₂O (< 5%) was produced at low temperatures (< 200 °C). Different from either Au/CeO₂ or Au/Al₂O₃, when CeO₂/Al₂O₃ was used as the support, the catalytic activities of gold at low temperatures were enhanced greatly. For example, the maximum NO conversion to N₂ over the 1.0%Au/16%CeO₂/Al₂O₃ was 46% at 250 °C, and N₂O formation was negligible in the whole temperature range. Obviously, the high selectivity to N₂ obtained on the Au/CeO₂/Al₂O₃ seems to be associated with the presence of the composite support CeO₂/Al₂O₃. It has been suggested that ceria is able to promote NO reduction to N₂O via the following route (25):



Consequently, a significant proportion of the N₂O formed on the Au/CeO₂ sample may be related to the oxygen vacancies in the CeO₂ support: but with Au/Al₂O₃, the formation of N₂O may follow a different path where a dissociative adsorption of NO on gold particles is involved (26,27). When a CeO₂/Al₂O₃ composite was employed as the support, the decreased oxygen vacancies can only partly explain the negligible production of N₂O (9). Other reasons may lie in the synergistic effect between Al₂O₃ and CeO₂ and these interpretations need to be further explored.

On the other hand, we can see from Figure 6C that C₃H₆ conversions were largely promoted by the presence of CeO₂. For example, a complete conversion of C₃H₆ was obtained

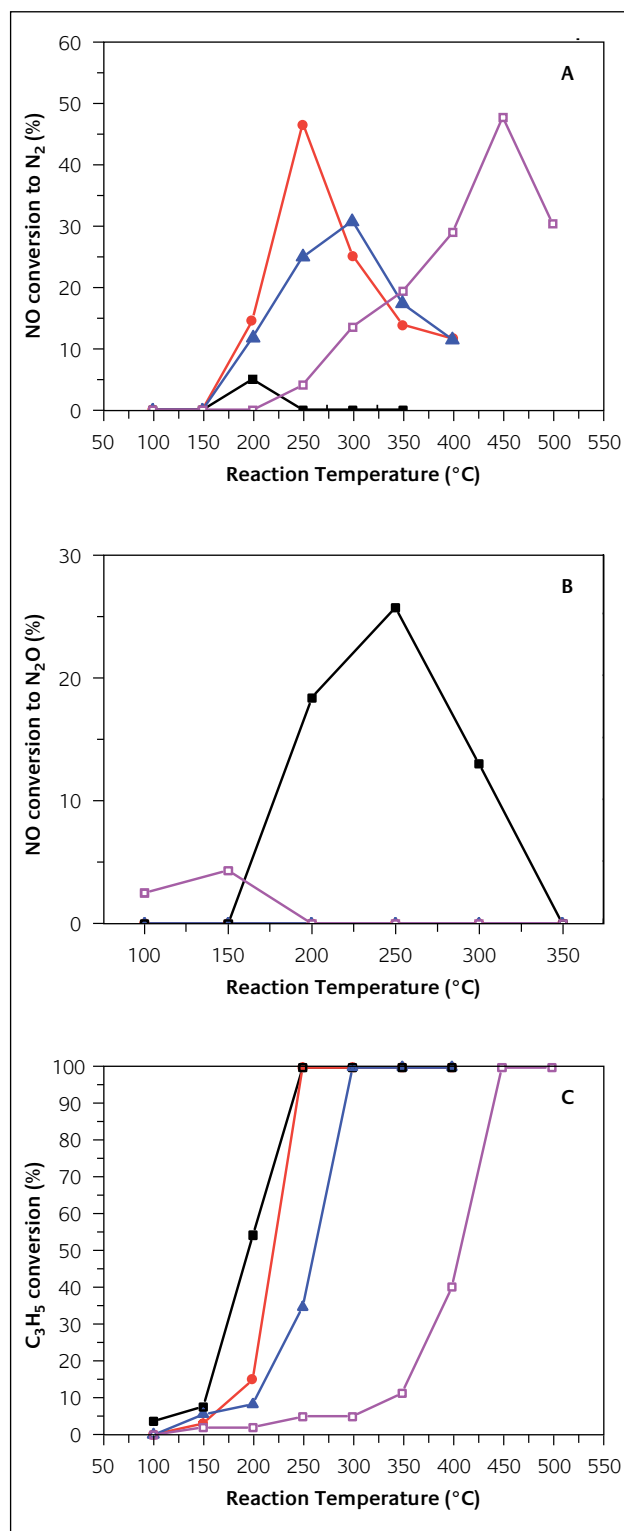


Figure 6

Reaction temperature dependence of NO conversion to N₂ (A) and N₂O (B) and C₃H₆ conversion to CO₂ (C) over 0.15g 1.4%Au/CeO₂ (■), 1.0%Au/16%CeO₂/Al₂O₃ (●), 0.9%Au/5%CeO₂/Al₂O₃ (▲) and 0.6%Au/Al₂O₃ (□). Feed conditions: 1000ppm NO, 1000ppm C₃H₆, 5% O₂ and He balance (vol%), total flow rate = 100ml min⁻¹.

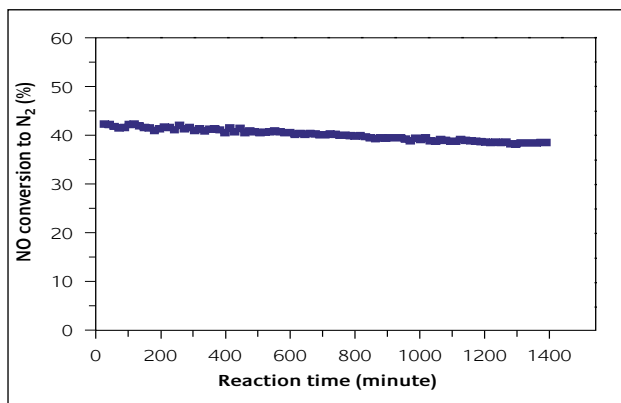


Figure 7

NO conversion to N_2 over 1.0%Au/16%CeO₂/Al₂O₃ catalyst as a function of reaction time at 250 °C.

at 250 °C over the Au/16%CeO₂/Al₂O₃, while it was realized at 450 °C over the Au/Al₂O₃. Comparing Figure 6A with Figure 6C, it can be seen that the maximum NO conversions are always associated with the complete conversion of C₃H₆. In agreement with our observations, Gluhoi et al. also found that Au/CeO₂/Al₂O₃ catalyst performed very well for the propene oxidation reaction (28). Such a high activity of the Au/16%CeO₂/Al₂O₃ in the complete oxidation of propene led to a low selectivity of C₃H₆ towards NO reduction. In fact, the selectivity of C₃H₆ towards NO reduction at 250 °C was only 23%.

Additionally, with a difference in the ceria content, the catalytic activity differs slightly. The sample with larger proportion of ceria (1.0%Au/16%CeO₂/Al₂O₃) shows higher catalytic activity, which may be related with the fact that Au/CeO₂ is more active than the Au/Al₂O₃ for propene oxidation (Figure 6C).

The stability of Au/16%CeO₂/Al₂O₃ was also investigated. From Figure 7, we can see that after a 1350min-run, the NO conversion only slightly dropped from 42% to 39%, indicating good stability. The presence of ceria prevents the agglomeration of gold, which is the main reason for the improved stability.

It is known that both SO₂ and water vapour are present in automotive emissions. It was, therefore, important to investigate the effect of these two components in the feed stream on the catalytic performance of our Au/CeO₂/Al₂O₃ sample. Figure 8 illustrates the conversions of NO and C₃H₆ with reaction temperature over the Au/16%CeO₂/Al₂O₃ in the presence of 2% water vapour or 20 ppm SO₂, and also in the simultaneous presence of the two components. Compared with the dry feed gas, it is interesting that the NO conversions in the low temperature range (100-200°C) were enhanced by the presence of moisture in the feed gas, whereas they were decreased at 250°C. The positive effect of H₂O on the NO conversion over the Au/CeO₂/Al₂O₃ at low temperatures is very similar to the case of CO oxidation over Au/Al₂O₃, which may be related to the creation of active Au species promoted by H₂O (18,29). Different from the influence of moisture, the presence of 20 ppm SO₂ greatly widened the temperature

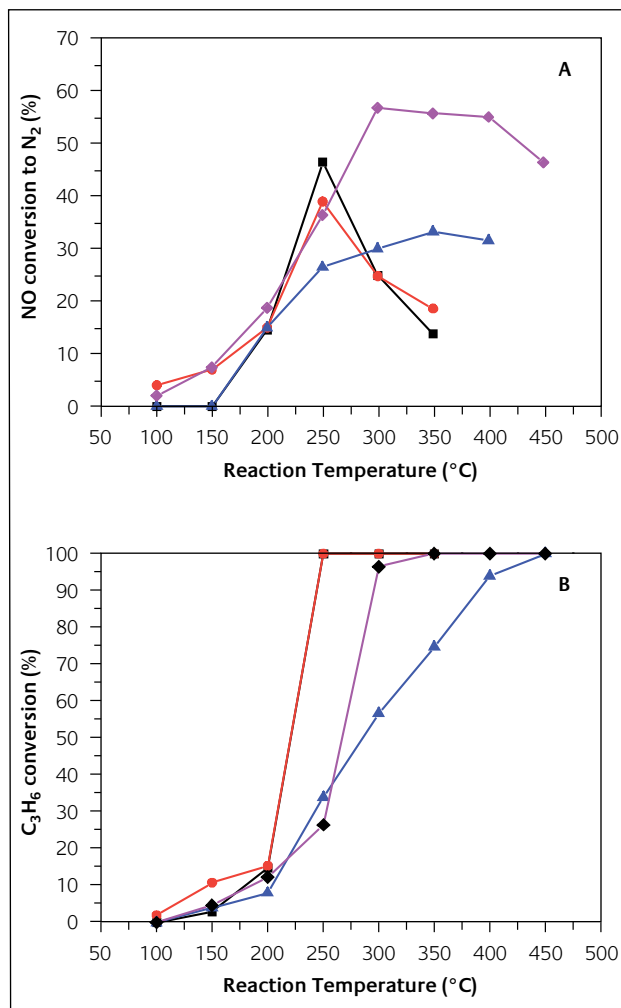


Figure 8

Reaction temperature dependence of NO conversions to N_2 (A) and C₃H₆ conversions (B) over 0.15g 1.0%Au16% /CeO₂/Al₂O₃ catalyst under the absence (■) or presence of 2%H₂O (●) or 20ppmSO₂ (▲) or simultaneous presence of 2%H₂O and 20ppmSO₂ (◆) in the feed stream. Gas composition: 1000ppm NO+ 1000ppm C₃H₆ +5%O₂, He as a balance.

window in spite of the fact that the maximum NO conversion decreased from 46% to 33%. To our surprise, under the simultaneous presence of 2% water vapor and 20 ppm SO₂, the NO conversions to N_2 were significantly increased, with the maximum NO conversion of 56% at 300 °C. Meanwhile, the temperature window was largely widened (250~450 °C). From Figure 8B, we can see that the C₃H₆ conversions were largely decreased by the addition of SO₂, suggesting that the presence of SO₂ suppress the combustion of C₃H₆ by O₂ and increases the selectivity of C₃H₆ towards NO reduction. It has been reported that the tolerance of metal oxide-based catalysts to SO₂ presence in the feed depends on the type and oxidation state of the deposited metal, and the nature of the support (30,31). In the case of Au/CeO₂/Al₂O₃, the enhanced activity and selectivity obtained by the addition of SO₂ may be caused by the selective or preferential poisoning of active sites for C₃H₆ combustion. This result provides some hints that NO reduction and C₃H₆ combustion occur at different sites.

In summary, the modification of alumina support with the ceria greatly improved the catalytic performance of gold particles in the NO reduction with propene. From the above XRD, TEM and TPR characterizations, we know that ceria was highly dispersed onto the alumina support, and this results in the easy reduction of not only surface ceria but also subsurface ceria. It has been suggested that the reduction of subsurface ceria is associated with the creation of oxygen vacancies, and gold preferentially deposited onto these sites helped by the strong interaction between the oxygen vacancies and gold particles. Therefore, the superior behaviour of Au/CeO₂/Al₂O₃ can be attributed to the improved interaction between gold and ceria particles. Such a catalytic performance is superior to that of Pt-group metal catalysts (1-5), on which a significant amount of N₂O (about 30%) was formed under similar conditions. Such a high catalytic activity and selectivity to N₂, combined with the excellent resistance to poison by water vapour and sulfur dioxide, makes Au/CeO₂/Al₂O₃ catalysts promising candidates for an effective 'cold start' application.

Conclusions

Highly dispersed ceria particles on alumina were prepared by impregnation, and then gold particles were deposited on this CeO₂/Al₂O₃ composite support. HRTEM-EDX measurements indicated that gold was preferentially deposited onto the ceria particles due to the improved interaction between gold and ceria nanoparticles. The Au/CeO₂/Al₂O₃ exhibited high activity and selectivity to N₂ at low temperatures, as well as good stability and resistance to poisoning by water and sulfur dioxide. These characteristics makes this catalyst a promising candidate for solving 'cold-start' problems in automobile emission control.

Acknowledgements

Supports of National Science Foundation of China (NSFC) for Distinguished Young Scholars (No. 20325620) and NSFC grant (No.20673116) are gratefully acknowledged

About the authors



Professor Tao Zhang is the Director of Dalian Institute of Chemical Physics, Chinese Academy of Sciences. His research interests are in heterogeneous catalysis, particularly in environmental catalysis.

References

- 1 A. Obuchi, A. Ohi, M. Nakamura, A. Ogata, K. Mizuno and H. Ohuchi, *Appl. Catal. B*, 1993, **2**, 71
- 2 R. Burch and T.C. Watling, *Appl. Catal. B*, 1997, **11**, 207
- 3 P. Denton, A. Giroir-Fendler, H. Praliaud and M. Primet, *J. Catal.*, 2000, **189**, 410
- 4 E. Seker and E. Gulari, *J. Catal.*, 2000, **194**, 4
- 5 R. Burch and D. Ottery, *Appl. Catal. B*, 1997, **13**, 105
- 6 M. Haruta, N. Yamada, T. Kobayashi and S. Iijima, *J. Catal.*, 1998, **115**, 301
- 7 A. Ueda, T. Oshima and M. Haruta, *Appl. Catal. B*, 1997, **12**, 81
- 8 A. Ueda and M. Haruta, *Gold Bull.*, 1999, **32**, 3
- 9 A. Trovarelli, *Catal. Rev. - Sci. Eng.*, 1996, **38**, 439
- 10 R. Dictor and S. Roberts, *J. Phys. Chem.* 1989, **93**, 5846
- 11 A. Martinez-Arias, M. Fernández-García, L.N. Salamanca, R.X. Valenzuela, J.C. Conesa and J. Soria, *J. Phys. Chem. B*, 2000, **104**, 4038
- 12 M.A. Centeno, P. Malet, I. Carrizosa and J.A. Odriozola, *J. Phys. Chem. B*, 2000, **104**, 3310
- 13 M.A. Centeno, C. Portales, I. Carrizosa and J.A. Odriozola, *Catal. Lett.*, 2005, **102**, 289
- 14 M.A. Centeno, M. Paulis, M. Montes and J.A. Odriozola, *Appl. Catal. A*, 2002, **234**, 65
- 15 J. Soria, J.M. Coronado and J.C. Conesa, *J. Chem. Soc. Faraday Trans.*, 1996, **92**, 1619
- 16 C. Morterra, V. Bolis and G. Magnacca, *J. Chem. Soc. Faraday Trans.*, 1996, **92**, 1991
- 17 Z. Yan, S. Chinta, A.A. Mohamed, J. P. Fackler, Jr. and D.W. Goodman, *J. Am. Chem. Soc.*, 2005, **127**, 1604
- 18 C.K. Costello, M.C. Kung, H.-S. Oh, Y. Wang and H.H. Kung, *Appl. Catal. A*, 2002, **232**, 159
- 19 S.-Y. Lai, Y. Qiu and S. Wang, *J. Catal.*, 2006, **237**, 303
- 20 H.C. Yao and Y.F. Yao, *J. Catal.*, 1984, **86**, 254
- 21 J. Guzman, S. Carrettin and A. Corma, *J. Am. Chem. Soc.*, 2005, **127**, 3286
- 22 P. Concepción, S. Carrettin and A. Corma, *Appl. Catal. A*, 2006, **307**, 42
- 23 C. Milone, M. Fazio, A. Pistone and S. Galvagno, *Appl. Catal. B*, 2006, **68**, 28
- 24 S. Scire, S. Minico, C. Crisafulli, C. Satriano and A. Pistone, *Appl. Catal. B*, 2003, **40**, 43
- 25 A. Martinez-Arias, J. Soria, J.C. Conesa, X.L. Seoan, A. Arcoya and R. Cataluna, *J. Chem. Soc. Faraday Trans.*, 1995, **91**, 1679
- 26 B.K. Cho, B.H. Shanks and J.E. Bailey, *J. Catal.*, 1989, **115**, 486
- 27 R. Burch, P.J. Millington, and A.P. Walker, *Appl. Catal. B*, 1994, **4**, 65
- 28 A.C. Gluhoi, N. Bogdanchikova and B.E. Nieuwenhuys, *J. Catal.*, 2005, **229**, 154
- 29 H.-S. Oh, C.K. Costello, C. Cheung, H.H. Kung and M.C. Kung, *Stud. Surf. Sci. Catal.* 2001, **139**, 375
- 30 E.A. Efthimiadis, G.D. Lonta, S.C. Christoforou and I.A. Vasalos, *Catal. Today*, 1998, **40**, 15
- 31 G. Zhang, T. Yamaguchi, H. Kawakami and T. Suzuki, *Appl. Catal. B*, 1992, **1**, L15